# Influence of the relative humidity and H2S -SO2 polluted air on the fretting wear behavior of silver-plated electrical contacts

F. Pompanon, Siegfried Fouvry, O. Alquier

# Influence of the relative humidity and $H_2S$ - $SO_2$ polluted air on the fretting wear behavior of silver-plated electrical contacts

F. Pompanon[1], S. Fouvry[1*], O. Alquier[2]

[1]LTDS, CNRS UMR 5513, Ecole Centrale de Lyon,

36 av Guy de Collongue, 69134 Ecully Cedex,

France

[2] PSA Groupe,

78943 Vélizy – Villacoublay Cedex,

France

*Corresponding author: siegfried.fouvry@ec-lyon.fr

*Abstract*— The use of connectors in electrical devices for automotive industry has significantly increased during the last decades. These connectors need to keep low and stable electrical contact resistance (ECR) otherwise disconnects may occur inducing critical failures. Close to the engine, these connectors are subjected to vibrations inducing fretting wear damage. The aim of this study is to investigate the influence of relative humidity and the presence of pollutant sulfurous gases ($H_2S$, $SO_2$) on the silver-plated electrical contact resistance (ECR) behavior. The ECR fretting endurance Nc (i.e. when $\Delta R > \Delta Rth = 4$ m$\Omega$) displays a fast increase above $RH_{th(Air)=}50\%$. The debris layer becomes more conductive so a larger wear volume is required to reach the ECR failure. At the same time, the debris layer becomes more cohesive and the wear rate decreases. Alternatively, synergic interaction between $H_2S$, $SO_2$ gases and relative humidity above $RH_{th(Air\&S)} = 60\%$ leads to the formation of lubricating $Ag_2S$ sulphide and $Ag_2SO_4$ sulphate tribofilm which, by decreasing the friction coefficient and the silver layer wear rate, sharply increases the ECR endurance. Finally, using simple explicit formulations, both ECR endurances under polluted and non-polluted air are formalized.

Keywords: $H_2S$ $SO_2$ gases, fretting wear, electrical contact resistance, silver coating, humidity, sulfurous gases.

## 1. Introduction

In automotive industry, the use of connectors for electrical devices has significantly increased over the past few decades. These connectors must provide a low and stable electrical contact resistance (ECR) otherwise disconnects may occur causing critical failures (Fig. 1). However, due to their working environment (car engine), they are subjected to vibrations which induce fretting micro-displacements in the electrical contacts. Fretting damage promotes the formation of an oxide debris layer leading to electrical failures.

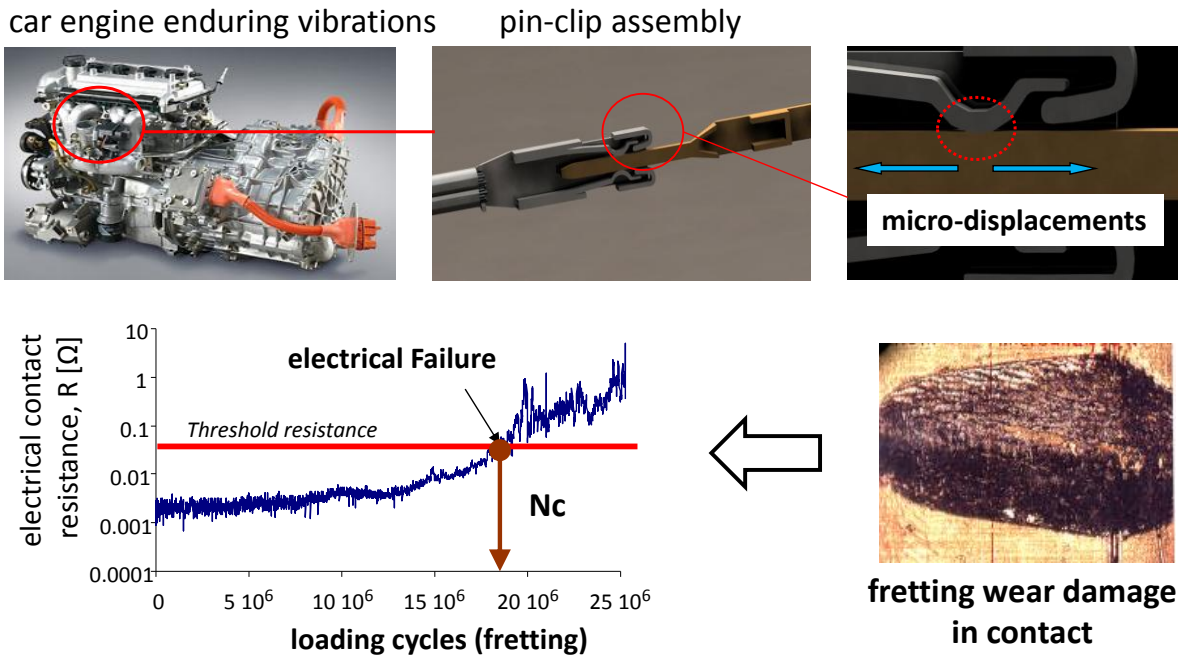


*Fig. 1: Illustration of the fretting wear damage in electrical contact (connectors).*

Since the first studies realized by Antler [1], [2], the degradation of electrical contacts has been extensively investigated [3-11] in order to determine the damage mechanisms and to identify palliative solutions. The most efficient method to reduce fretting wear damage consists in applying noble coatings. Gold layers are currently the most used coatings due to their high electrical conductivity and high corrosion resistance [12-14]. However, due to the expensive price of gold, silver is now considered as a promising alternative [15-17]. Nevertheless, the behavior of silver coatings has to be studied under severe environmental conditions (temperature, humidity, pollutant gases) in order to ensure that silver-plated coatings are reliable enough to substitute gold coatings in most environmental situations.

Various investigations, led by Hannel et al. [18] and Kassman-Rudolphi and Jacobson [19], [20], underlined the influence of sliding regimes on electrical connector performances. Hence, as long as partial slip fretting conditions are maintained, an inner metal/metal stick zone operates, promoting stable and low ECR and infinite electrical endurance (i.e. Nc fretting cycles above which ECR overpasses $\Delta R_{th}$=4 mΩ threshold). In contrast, above the gross slip transition ($\delta^*_t$), the full sliding operating within the interface promotes surface wear and the formation of a low-conducting oxide debris layer leading to finite electrical endurance.

Numerous investigations were performed to correlate the surface degradation with the ECR evolution [17], [21], [22]. It was concluded that for noble coatings, the increase of the ECR is induced by the progressive elimination of the top silver or gold coating and the formation of a homogeneous insulating oxide debris layer.

Former investigations underline the beneficial effect of the relative humidity regarding ECR endurance of noble materials like silver [22]. Below RH=50%, the debris bed displays a powder structure favoring a fast debris ejection, rather high wear rates and consequently low ECR endurances. A smooth increase of Nc is however observed due to a lubricating effect of water. Above RH=50%, the moist atmospheres drastically reduce the wear rate promoting a fast rising of the ECR endurance.

In addition to humidity, electrical connectors are subjected to pollutant sulfurous gases present in the exhaust gases as sulfur dioxide $SO_2$ and hydrogen sulfide $H_2S$. In the case of silver contacts, the chemical reactions that may occur can be very damaging because silver is very susceptible to sulfidation. Hence, the aim of this work is to investigate this aspect, studying the synergic interactions between the relative humidity and the presence of sulfurous gases in polluted air.

## 2. Experimental details

### 2.1 Materials

The samples used in the present study are crossed cylinders with a homogenous Ag/Ag contact (i.e. similar upper and lower cylinders) (Fig. 2).

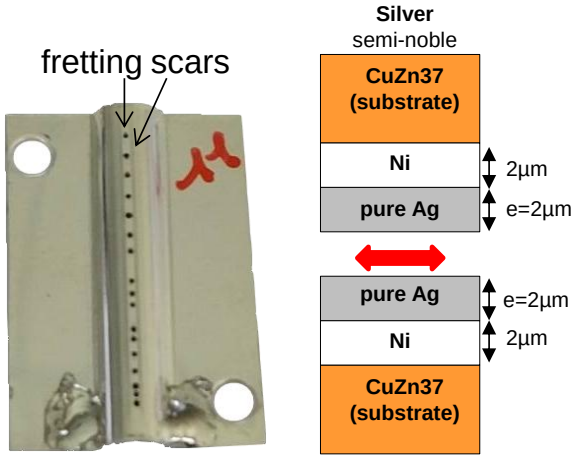


*Fig.2: Illustration of the studied CuZn37 (substrate)-Ni-Ag specimen fretted applying a crossed-cylinder contact configuration (by translating bottom and top specimens more than 15 tests can be performed using a single couple of specimens).*

The interface structure (Fig. 2) consists in a 37 wt.% zinc (CuZn37) brass alloy substrate onto which a 2 µm electrolytic nickel interlayer was deposited in order to limit copper diffusion. On this standard structure, a 2 µm pure silver layer was deposited using a dedicated electrolytic process.

## 2.2 Experimental procedure

Figure 3a illustrates the fretting test machine used in this investigation [17]. Fretting displacement (δ) was applied to the upper specimen using an electromagnetic shaker and measured using a high-resolution laser extensometer. The upper specimen holder was fixed to the shaker using flexure strips to guarantee the application of the normal force. The lower sample was fixed on the bottom specimen holder above which a piezoelectric load sensor allows the tangential force recording during the test. The normal force (P) is applied using a dead mass. The plotting of the Q-δ fretting loop (Fig. 3b) allows the determination of the friction energy (i.e. friction work) dissipated within the interface (Ed(J)) but also the estimation of the tangential force amplitude (Q*) as well as the effective sliding amplitude operating ($\delta_s^*$) which is measured from the fretting loop when the tangential force is zero (i.e. residual displacement measured on the fretting cycle reversing when Q = 0).

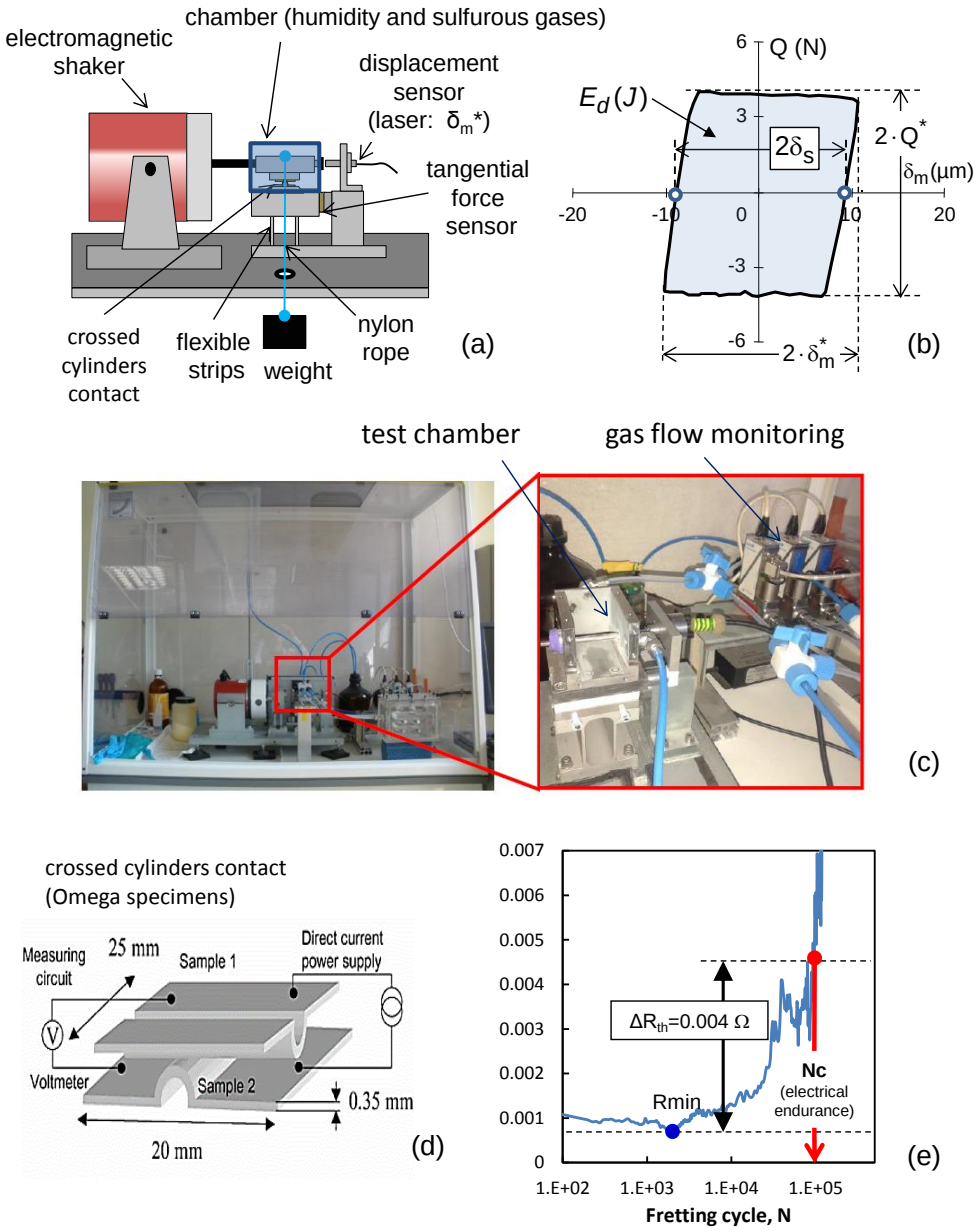


*Fig. 3: (a) Schematic illustration of the fretting test bench; (b) fretting loop analysis; (c) picture of the experimental set-up including gas and relative humidity monitoring;(d) illustration of the crossed-cylinders contact configuration and the "four-point" method used to measure the electrical contact resistance; (e) illustration of the determination of the electrical contact endurance Nc.*

Indeed, the applied displacement amplitude ($\delta^*$) is not equal to the sliding amplitude since a significant part of the displacement is accommodated by the elastic test accommodation [23]. Finally, the friction coefficient is given by:

$$\mu = \frac{Q*}{P} \qquad (1)$$

The experiment detailed in [17] and [22] has been updated to incorporate a chamber allowing the circulation of various sulfurous gases (Fig. 3c). The test system is equipped with $SO_2$ and $H_2S$ doped nitrogen bottles combined with a non-polluted bottle. These three gases are thus mixed and injected into a gas circulation system. The gas flows are controlled using servo valves to achieve the desired concentrations of sulfur contaminants in the fretting chamber related to the so-called "Air&S" polluted air atmosphere (i.e. [$H_2S$] = 0.5 ppm and [$SO_2$] = 1.2 ppm). Such [$H_2S$] and [$SO_2$] concentrations are representative of the testing conditions in automotive industry. An MST Satellite analyzer with an accuracy of 0.1 ppm is used to measure and control the $H_2S$ and $SO_2$ concentrations of the "polluted" air.

In order to carry out tests at various humidity levels, the air flow is transferred to a so-called "humidity chamber" where saturated saline solutions (NaCl, $K_2SO_4$ ...) allow reaching the desired level of relative humidity. Finally, the humid air flow (polluted or not polluted) is transferred to the test chamber.

A bypass system is also implemented on the test chamber to capture part of the exhaust polluted air toward the MST Satellite analyzer along with a relative humidity sensor to precisely control the air composition operating in the fretting test chamber.

### 2.3 Contact Configuration and Electrical Resistance Measurement

The contact assembly consists in a 90° crossed-cylinders (omega specimen) configuration with a 2.35 mm cylinder radius (Fig. 3d). According to the Hertzian theory, this contact configuration is equivalent to a sphere/plane contact with R = 2.35 mm. During the test, the electrical contact resistance was measured using a 4-wire method. A current source applied I =5 mA with 10 V voltage compliance while a μvoltmeter system measured the contact voltage at a resolution of 0.01 μV. This system makes it possible to measure the electrical resistance from $10^{-6}$ to $10^{3}$ Ω. As previously mentioned, under gross slip condition, fretting wear damage reduces the ECR endurance. To quantify this aspect, the number of fretting cycles needed to reach an electrical resistance fluctuation (from the minimum value measured during the test) overpassing a $\Delta R_{th}$=4 mΩ threshold is defined as Nc ECR endurance (Fig. 3e). Note that the ECR is established and the test is stopped when the electrical failure condition is satisfied during 500 consecutive fretting cycles otherwise the fretting test is continued until satisfying the effective failure condition. Monotonous ECR evolutions have been observed so that no false failures have been detected.

2.4 Test conditions

Similar contact loading conditions as those previously applied in [22] are considered. The normal force is kept constant at P=3 N as well as the temperature at T=25°C. A constant fretting sliding amplitude is imposed $\delta^*_s$=±9 µm, at a frequency f=30 Hz.

The sulfurous gases concentrations were measured and kept constant: [$H_2S$] = 0.5 ppm, [$SO_2$]= 1.2 ppm. The relative humidity (RH) is the only variable parameter. It is controlled using various NaCl, $K_2SO_4$ saturated saline solutions, for tests in polluted and non-polluted air, in a range from 10% to 75%. These experimental data will be compared with former "non-polluted air" conditions where the relative humidity was instead monitored using a climatic generator [22]. Climatic generator allows a better regulation of RH condition but cannot be used with corrosive $H_2S$ - $SO_2$ ambient.

For specific relative humidity conditions (i.e. RH=10, 50 and 60%) tests were duplicated 3 times and only one time for other conditions. Crossed omega configuration allows performing up to 10 tests per couple of specimens. Hence, less than 4 pairs of specimen were required for polluted and non-polluted air investigation respectively (i.e. total number of 8 pairs for the study). Whether polluted or non-polluted air conditions, the tests were performed by increasing successively the RH condition so that dryer tests were never done on surfaces previously exposed to moister ambient.

## 3. Results

3.1 Influence of sulfurous gases on ECR resistance and friction behavior

Figure 4 illustrates the evolution of the electrical contact resistance and the coefficient of friction respectively as a function of the fretting cycles for "non-polluted air" for 3 relative humidity conditions RH = 10%, 50% and 70%. Note that all the tests have been stopped at the ECR failure condition (i.e. Nc when $\Delta R > \Delta Rth$=4 mΩ).

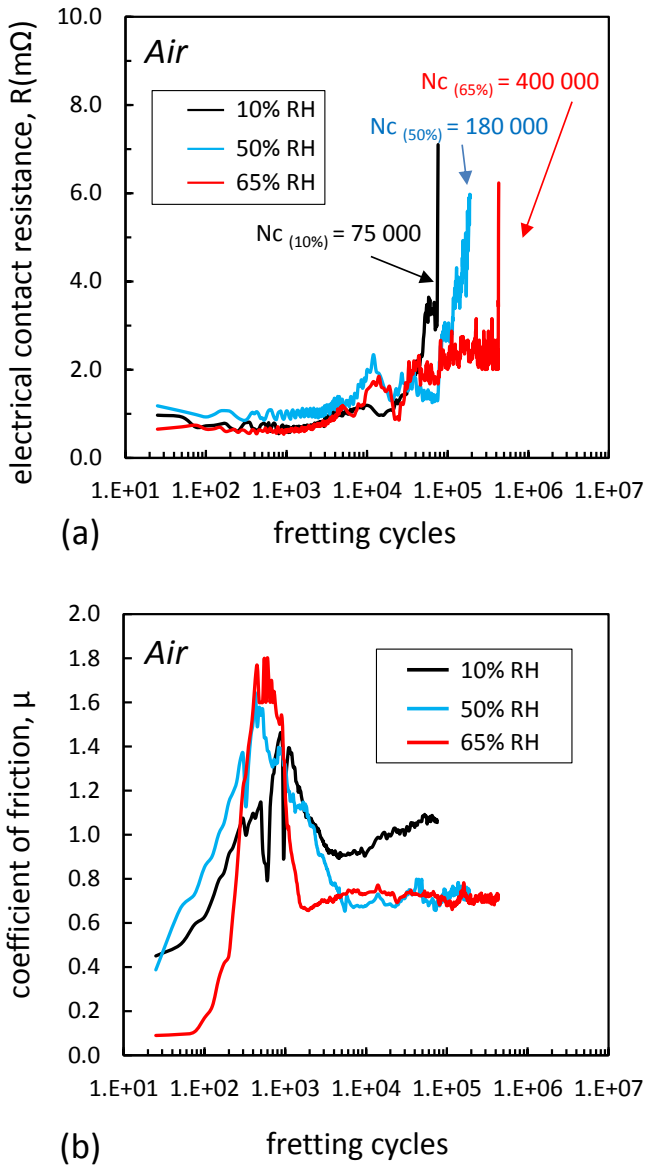


*Fig. 4: Fretting wear response of Ag-platted coating for various relative humidity under non-polluted atmosphere (Air): (a) evolution of the electrical contact resistance; (b) evolution of the coefficient of friction (P=3 N, T=25 °C, $\delta_s^*$= ±9 µm, f=30 Hz).*

As detailed in [22], the higher the relative humidity the longer the ECR endurance. During the first part of the test, ECR remains low and stable then, when the fretted interface is damaged leading to the formation of an insulating oxidized debris layer, the ECR displays an exponential rising until the electrical failure. The ECR evolution can be correlated to the friction response. After a fast elimination of organic contaminants, the direct interaction between Ag layers promotes metal transfers and a very sharp rising of the coefficient of

friction up to 1.6 to 2. These direct metal interactions also provide low and stable ECR values. However, after few hundreds of cycles, the formation of the first wear debris tends to accommodate the interface and the coefficient of friction drops until 1 for dry condition (10%) and around 0.7 for moist situations. The ECR is maintained low during few thousands of fretting cycles until the noble Ag wear debris particles are progressively replaced by insulating Nickel and Copper oxide wear debris. Under dry condition (RH= 10%), the powder structure of worn debris favors a faster debris ejection process and therefore a faster wear rate which consequently induces rather short ECR endurance. Above RH=50%, the debris layer becomes more cohesive and more compliant. The debris ejection rate (i.e. wear rate) decreases yet the higher electrical conductivity of the debris bed can explain the longer ECR endurances observed (Fig. 4, RH =65%). Figure 5 compares the evolution of the same silver platted interface varying the relative humidity under polluted air (i.e. [$H_2S$] = 0.5 ppm and [$SO_2$] = 1.2 ppm gases).

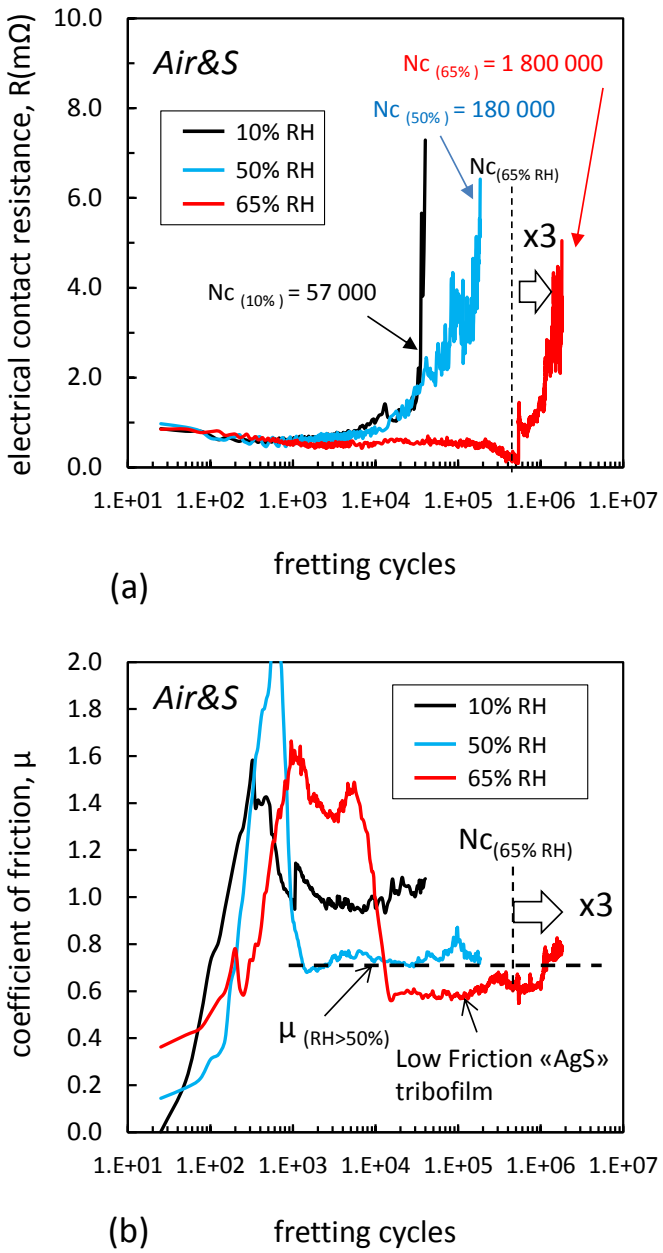


*Fig. 5: Fretting wear response of Ag-platted coating for various relative humidity conditions under polluted atmosphere (Air&S: [$H_2S$] = 0.5 ppm and [$SO_2$] = 1.2 ppm): (a) evolution of the electrical contact resistance; (b) evolution of the coefficient of friction (P=3 N, T=25 °C, $\delta_s^*$= ±9 µm, f=30 Hz).*

Similar evolutions as those observed under "non-polluted" air are detected for RH = 10% and 50%. This suggests that for medium low RH conditions, $H_2S$ and $SO_2$ contaminants play a minor effect regarding the tribological response and the electrical contact resistance behavior. A significant difference is however observed for the higher RH=65% condition. The friction

coefficient stabilizes at a lubricious 0.6 plateau from $10^4$ to $10^6$ fretting cycles before rising up to 0.7 friction level previously observed for non-polluted air conditions. The 0.6 friction period suggests synergic interactions between high relative humidity (65% RH) and $H_2S$ and $SO_2$ contaminants to form a protective tribofilm layer.

3.2 Evolution of ECR resistance endurance (Nc)

This investigation was generalized varying the relative humidity from 5 to 90%. As before, all the tests have been stopped at the ECR failure condition. Figure 6 compares the evolution the Nc versus the applied relative humidity for non-polluted (Air) and polluted air (Air&S) conditions. Note that the non-polluted air results given by NaCl-$K_2SO_4$ are similar to those provided by the climatic chamber [22] confirming the reliability of saline solution experiments. For non-polluted air a bilinear rising evolution is observed marking a transition around $RH_{th\_Nc(Air)}$= 50%. The ECR endurance under polluted air displays a similar evolution until $RH_{th\_Nc(Air\&S)}$= 60%. Above this threshold, a discontinuous increase of the Nc is detected suggesting a synergic interaction between the highest relative humidity conditions and the presence of $H_2S$ and $SO_2$ contaminants.

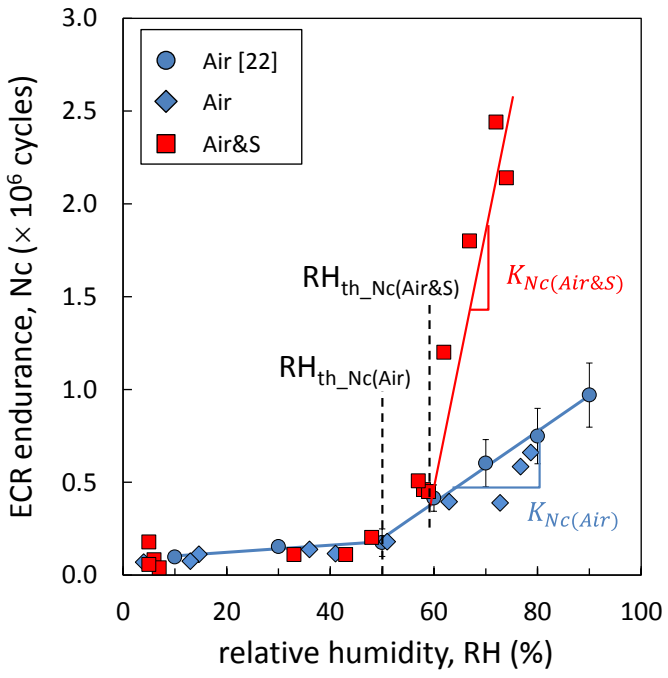


*Fig. 6: Evolution of the ECR endurance (Nc) versus RH under non-polluted (Air) and polluted (Air&S: [$H_2S$] = 0.5 ppm and [$SO_2$] = 1.2 ppm) atmospheres (P=3 N, T=25 °C, $\delta_s^*$=±9 µm, f=30 Hz).*

These typical ECR can be quantified by the slope of the linear approximations. For non-polluted air and RH values smaller than $RH_{th\_Nc(Air)}$ = 50%, this latter is around $K_{Nc(Air)}$ = 1 900 cycles/ RH(%) and rises to 19 000 cycles/RH(%) for moister atmospheres. Under polluted air condition, a similar tendency as non-polluted air is observed up to $RH_{th\_Nc(Air\&S)}$ = 60%, above which it rises up to $K_{Nc(Air\&S)}$ ≈150 000 cycles/RH(%) which is 8 times higher than the equivalent value measured for non-polluted air conditions.

3.3 Evolution of the coefficient of friction up to ECR failure

This typical evolution of ECR endurance can be compared versus the corresponding evolution of the mean friction coefficient averaged over the whole test duration (Fig. 7). As detailed previously in [22], the friction coefficient μ displays a sharp reduction from dry air (RH = 5%) to more humid air around RH = 30%. This decrease is related to a liquid lubrication process [22] due to the formation of a water nano-film at the surface [24]. This induces a reduction of the friction dissipation and explains the smooth Nc rising below RH = 50% (domain (I)). Then, above RH = 30% and for non-polluted air condition, the mean coefficient of friction stabilizes around 0.7.

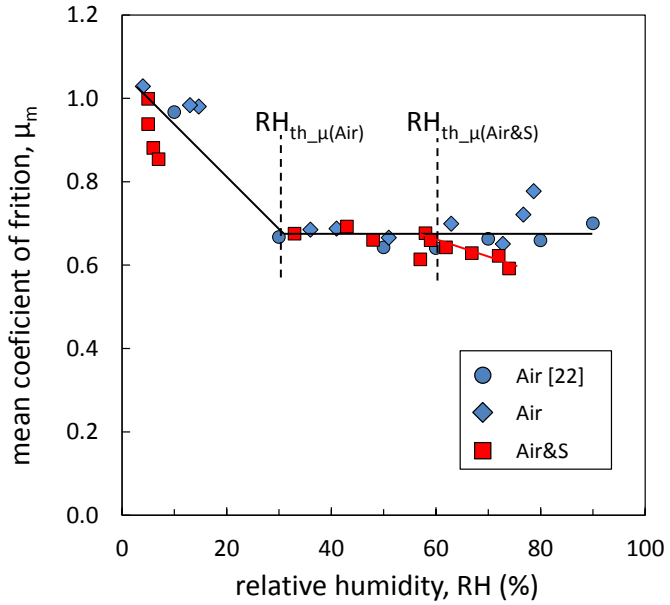


*Fig. 7: Evolution of the mean coefficient of friction $\mu_m$ averaged until Nc as a function of RH for non-polluted (Air) and polluted (Air&S: $[H_2S]$ = 0.5 ppm and $[SO_2]$ = 1.2 ppm) atmospheres (P=3 N, T=25 °C, $\delta_s^*$= ±9 μm, f=30 Hz).*

A similar tendency is observed for polluted air until $RH_{th\_\mu(Air\&S)=}$ 60%. Above this threshold value, the mean friction value drops compared to the non-polluted ambient down to 0.6 around RH=75%. This typical friction evolution is better interpreted by the dynamical evolution of the coefficient of friction versus fretting cycles. The friction curves at RH=10% under non-polluted air (Fig. 4b) and polluted air (Fig. 5b) are similar. They display a peak evolution up to 1.5 during the first thousand cycles then stabilize at μ=1 friction plateau which also corresponds to the mean friction value displayed in Figure 7 for the dryest RH= 10% condition.

The analysis under moist conditions (i.e. RH=60%) underlines a significant difference between non-polluted and polluted air conditions (Fig. 8a). Under pure air a rather stable μ=0.75 "High Friction" plateau is observed until the ECR failure at Nc =0.8 $10^6$ cycle. It corresponds to the formation of a more compliant agglomerated oxides and a potentially hydrated third body layer [22].

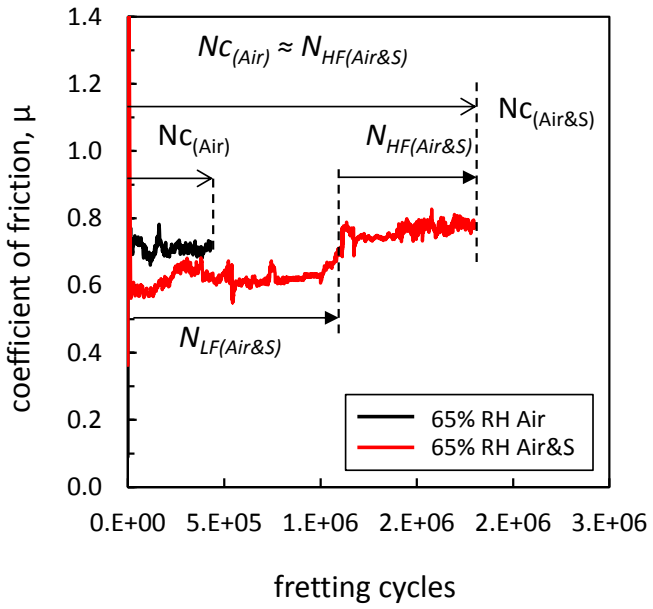


*Fig. 8: Evolution of the coefficient of friction until the ECR failure (Nc) under moist RH=65% condition for non-polluted (Air) and polluted air (Air&S: [$H_2S$] = 0.5 ppm and [$SO_2$] = 1.2 ppm) atmospheres (P=3 N, T=25 °C, $\delta_s^*$ = ±9 μm, f=30 Hz).*

The evolution of the friction behavior under moist and polluted air is more complex. A "Low Friction" plateau at μ=0.6 is first observed during $N_{LF(Air\&S)}$= 1.2 $10^6$ cycles. Then the friction

coefficient suddenly rises up to the high friction plateau (μ=0.75) during approximately $N_{HF(Air\&S)}$ = 0.8 $10^6$ cycles until the ECR failure. It is interesting to note that the duration of this second high friction plateau is nearly equivalent to the one observed for non-polluted air before the ECR failure $N_{C(Air)}$. This discontinuous "staircase" evolution suggests the formation of a beneficial silver sulfurous lubricating compound which is progressively eliminated during the fretting wear process. However, as long as this latter is present in the interface, the silver coating is protected and the ECR failure is postponed in proportion.

Figure 9a compares the evolution of the coefficient of friction under polluted air for various relative humidity conditions. It confirms that the higher the relative humidity, the longer the initial low friction plateau and consequently the longer the total ECR endurance. The comparison with electrical resistance (Fig. 9b), suggests that when the low friction tribo-layer is decayed, the ECR which was previously low and stable, displays a discontinuous rising of about 1 mΩ followed by unstable evolution until the ECR failure.

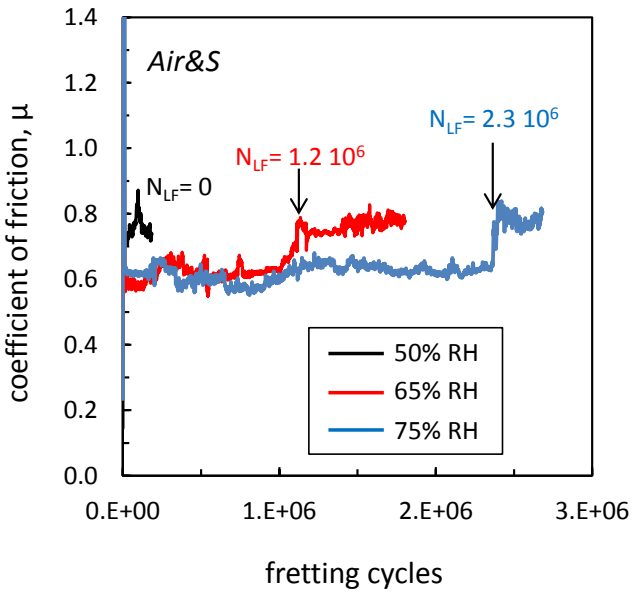


(a)

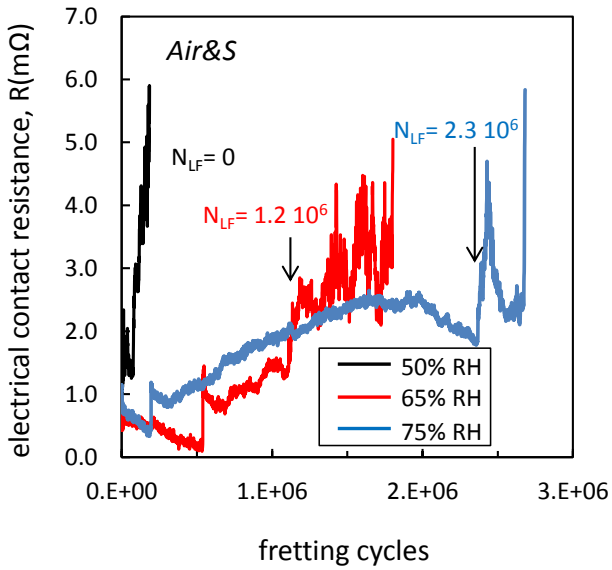


(b)

*Fig. 9: (a) Evolution of the coefficient of friction under polluted air (Air&S: [$H_2S$] = 0.5 ppm and [$SO_2$] = 1.2 ppm) until the ECR failure (Nc) as a function of the relative humidity; (b) Corresponding evolution of the electrical contact resistance (ECR) (P=3 N, T=25 °C, $\delta_s^*$=±9 µm, f=30 Hz).*

3.4 Evolution of the wear volume at the ECR failure

The surface wear analysis at the Nc ECR failure condition has been generalized to plot the evolution of the total wear volume $V_{Nc}$ (i.e. the sum of the upper and lower wear volumes) as a function of the applied relative humidity for polluted and non-polluted air conditions (Fig. 10).

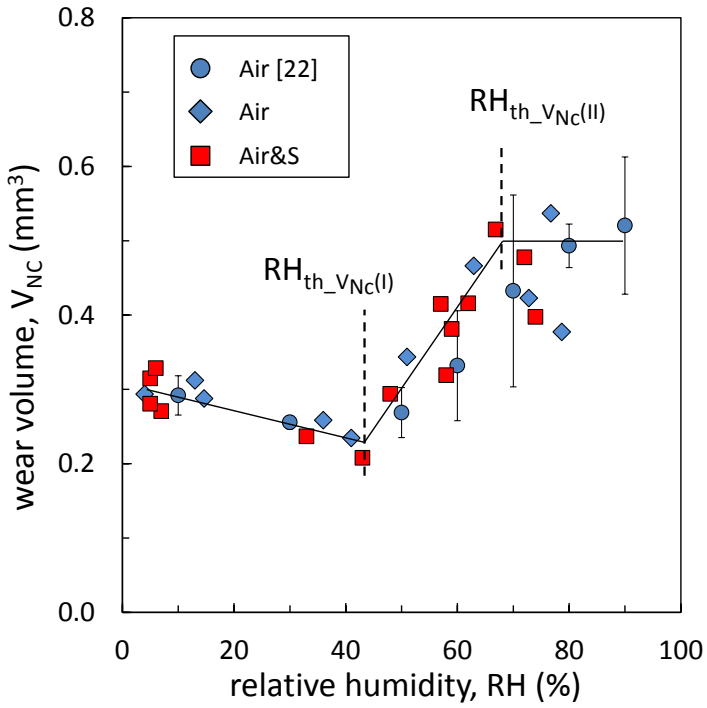


*Fig. 10: Evolution of the total wear volume at the ECR failure (Nc) as a function of RH for non-polluted (Air) and polluted air (Air&S :[$H_2S$] =0.5 ppm and [$SO_2$] =1.2 ppm) atmospheres (P=3 N, T=25 °C, $\delta_s^*$= ±9 µm, f=30 Hz).*

Similar evolutions are observed for both polluted and non-polluted air conditions suggesting that only the relative humidity is governing the wear volume damage. Under low and medium humidity levels (i.e. RH < $RH_{th\_VNc(I)} \approx 40\%$), $V_{Nc}$ remains almost stable and even displays a slight decrease until RH= 50%. However, above RH= $RH_{th\_VNc(I)}$, the threshold wear ($V_{Nc}$) displays a sharp quasi-linear increase until being stabilized above $RH_{th\_VNc(II)}$ = 75%.

3.5 Evolution of the wear rate

The ECR endurance appears dependent on the surface wear damage and therefore can be formalized as function of the wear volume which must be removed before reaching the ECR failure. To illustrate this aspect the Archard wear rate is computed for each test condition such that [25]:

$$K = \frac{V_{Nc}}{\sum W_{Nc}} \quad (2)$$

With $\sum W_{Nc}$ being the accumulated Archard work dissipated at Nc approximated by:

$$\Sigma W_{Nc} = 4 \times P \times \delta_S^* \times Nc \quad (3)$$

Figure 11 plots the log evolution of the Archard wear rate (K) versus the relative humidity for non-polluted and polluted air conditions. Regarding non-polluted air conditions, a smooth continuous decrease of the wear rate is observed. Polluted air condition displays a similar evolution up to $RH_{th\_K(Air\&S)}$ =60% above which a sharp drop is observed.

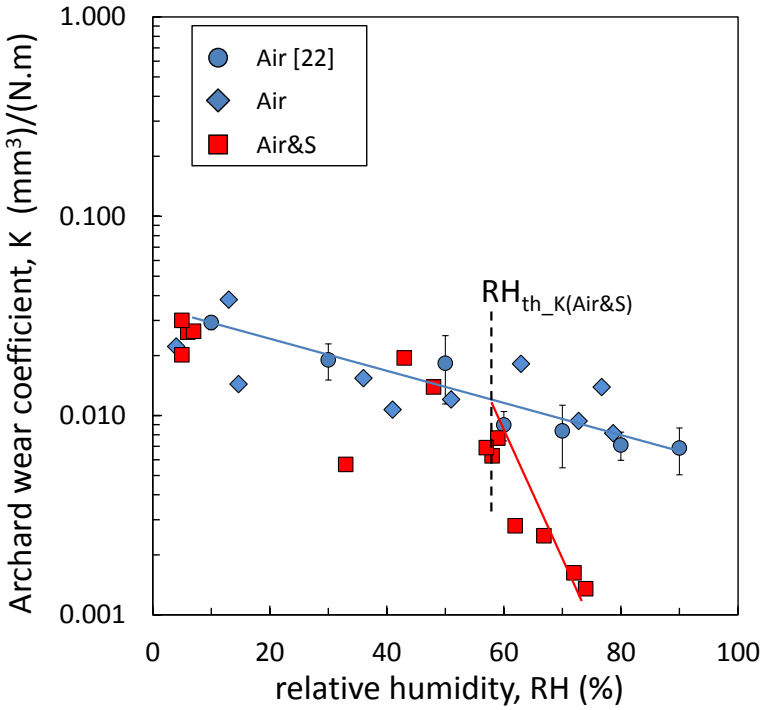


*Fig. 11: Evolution of the total wear volume at the ECR failure (Nc) as a function of RH for non-polluted (Air) and polluted air (Air&S: [$H_2S$] =0.5 ppm and [$SO_2$] =1.2 ppm) atmospheres (P=3 N, T=25 °C, $\delta_s^*$=±9 µm, f=30 Hz).*

## 4. Surface analysis

### 4.1. SEM, EDX and 3D surface expertise

Figures 12 details the fretting scar expertise of fretting contacts stopped just at the ECR failure condition. SEM and EDX observations have been performed at the contact opening whereas the 3D surface profiles were done after a 10-minute ultra-sonic ethanol bath cleaning to remove most of the wear debris remaining in the fretting scar.

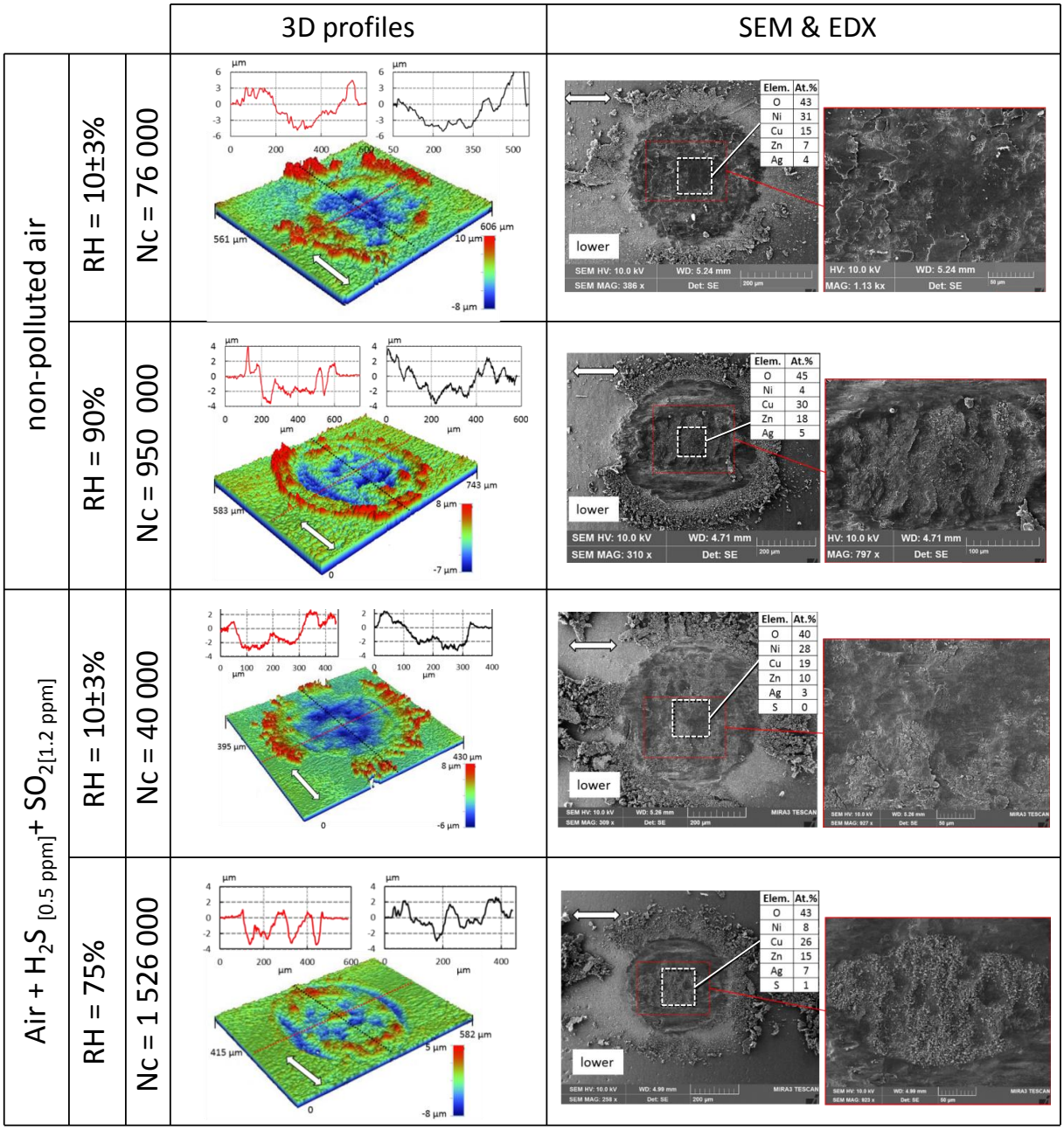


*Fig. 12: Fretting scar analysis at the Nc ECR failures for dry and moist conditions under non-polluted and polluted situations. SEM and EDX observations of the fretting scars were done at the contact opening whereas 3D surface profiles were performed after an ultra-sonic cleaning in an ethanol bath (EDX analysis were performed at 20 kV and results are in %atomic).*

No significant differences between fretting scar morphologies can be observed. The debris maintained within the interface displays a compacted morphology (i.e. platelet structure) whereas the debris observed outside the fretting scar presents a powder structure. This can be explained by the high hydrostatic pressures imposed within the contact which tend to compact

the debris bed whatever the relative humidity. It can be also assumed that the vacuum conditions required by SEM observations tends to dehydrate the less compacted wear debris expelled outside the contact so that it is difficult to distinguish a difference in the morphology between the debris formed under dry or moist atmospheres. Besides, these qualitative observations do not allow deliberating the thickness of the debris bed entrapped within the interface.

More interesting is the EDX semi-quantitative analysis of [Ag] and [O] concentrations which confirm that whatever the applied relative humidity under polluted or non-polluted air conditions, the ECR failure is effective when the [Ag]th - [O]th threshold criterion previously introduced in [17] is satisfied:

$$\text{Nc when } [Ag] < [Ag]_{th} \approx 5 \text{ At\%} \quad (4)$$

$$\text{And } [O] > [O]_{th} \approx 45 \text{ At\%} \quad (5)$$

This result is very important because it suggests that with a simple postmortem EDX expertise, we can know if the electrical contacts have reached the ECR failure or not.

Another interesting result concerns the [Ni]/[Cu] ratio which, under dry RH=10% condition, is around 2 and 1.5 for non-polluted and polluted air respectively. However it falls below 0.15 and 0.3 under moist conditions (RH > 70%). These results are consistent with the $V_{Nc}$ wear volume analysis (Fig. 10). The larger the relative humidity the larger the wear volume at the ECR failure so the smaller the [Ni]/[Cu] ratio. This also indirectly supports the assumption that under dry condition, lower electrical conductivity of debris layer implies that the ECR decay is reached whereas the fretted interface is still operating within the Ni sublayer. Alternatively, under moist atmospheres, the increase of the electrical conductivity of the debris bed and possibly the formation of conductive hydrates, suggest that thicker third body layer, consisting of insulating cupper oxides and therefore larger wear volume must be formed to satisfy the ECR failure condition.

An alternative strategy to demonstrate the thicker third body thickness at the ECR failure under moist atmospheres consists in applying the methodology introduced by Arnaud et al. [26]. Hence, by superimposing the uncorrected 2D profiles of cleaned surfaces in contact, it is possible to extrapolate the gap between the two surface profiles which in fact corresponds to the debris layer previously entrapped within the interface and removed by the surface cleaning. Figure 13 compares the superposition of worn profiles for dry (RH=10%) and moist

condition (RH=75%). The given results concern polluted air experiments but similar conclusions have been derived for non-polluted situation. For RH = 10%, the upper and lower profiles match perfectly. Thus, the third body thickness is very thin about 0.5 to 1 µm. However, for RH= 75%, an important gap is observed which suggests a maximum third body thickness up to 8 µm.

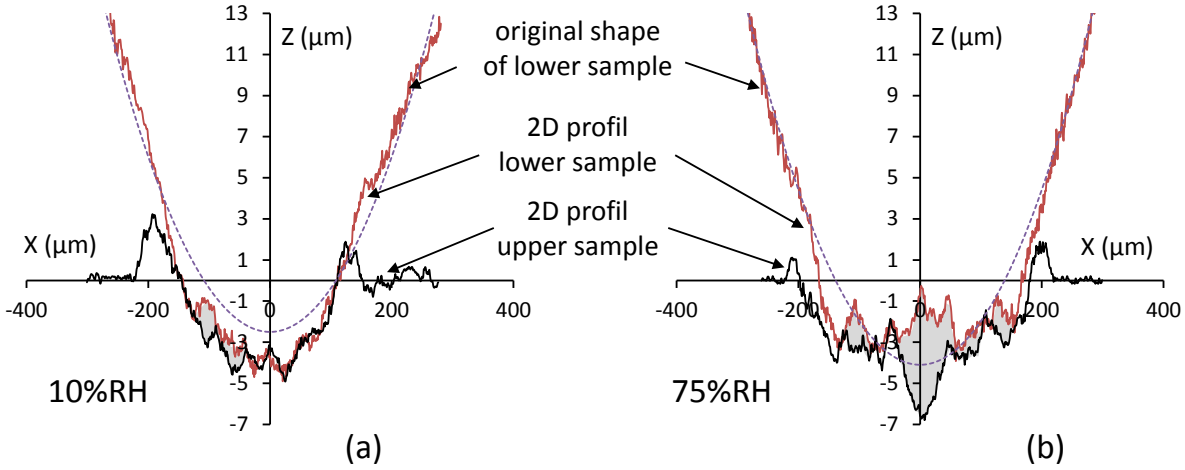


*Fig. 13: Estimation of the debris layer (gap) by superposing the fretting scar profiles (a) under dry condition (RH=10%) and (b) moist atmosphere (RH= 75%) polluted air condition with [$H_2S$] = 0.5 ppm and [$SO_2$] = 1.2 ppm (P=3 N, T=25 °C, $\delta_s^*$= ±9 µm, f= 30 Hz).*

4.2 EDX & XPS investigation of the Ag-S lubricious tribofilm

Above $RH_{th(Air\&S)}$=60%, a sharp increase of the Nc ECR endurance is observed for the polluted air atmosphere (Fig. 6). This increase does not seem to be induced by a modification of the wear volume required to reach the electrical failure (Fig. 10). This indirectly suggests that sulfur elements do not modify the electrical conductivity of the third body layer, at least for the studied conditions, since similar surface damage (i.e. debris layer thicknesses) needs to be achieved to reach the ECR decay.

The fast rising of Nc above $RH_{th(Air\&S)}$=60% seems to be rather explained by a fast drop of the wear rate as illustrated in Fig 11. This latter is not related to an average reduction but rather explained by a sequential process. When the protective Ag-S tribofilm is finally eliminated after $N_{LF(Air\&S)}$ fretting cycles, a similar behavior as that observed for non-polluted air is observed inducing a staircase 0.75 friction rising and a faster surface damage process. Hence, by delaying the contact degradations, this lubricious Ag-S tribofilm significantly reduces the

global wear rate and sharply increases the ECR endurance. To examine the nature of this lubricious tribofilm, an interrupted test stopped after 8 $10^5$ cycles (N/Nc ≈ 2/5), was done and analyzed (Fig. 14).

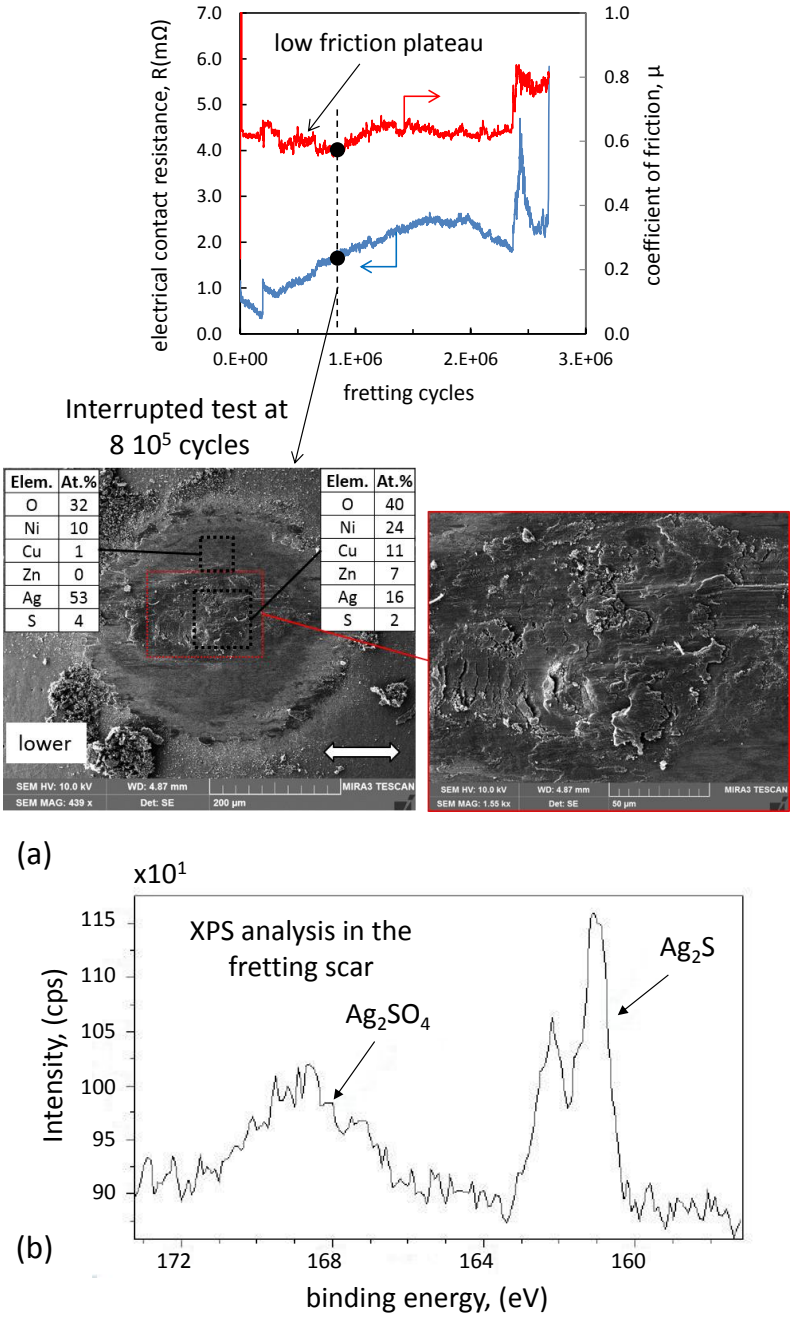


*Fig. 14: (a) SEM, EDX and (b) XPS analysis of Ag fretting scar under polluted air ([$H_2S$] = 0.5 ppm and [$SO_2$] = 1.2 ppm) and elevated RH= 75% condition stopped after N= 8 $10^5$ fretting cycles to characterize the lubricious μ=0.6 sliding plateau (P=3 N, T=25 °C, $\delta_s^*$ = ±9μm, f=30 Hz).*

EDX analysis underlines higher concentrations of sulfur than those at the failure condition (Fig. 12), yet, they are still relatively low. The concentration of sulfur in the center of the contact is around [S] = 2 at.% for a silver concentration of 16 at.% whereas at the contact edges, where the surface degradations are lower, they reach 4 and 53 at.% respectively. After this analysis, it can be hypothesized that $H_2S$ and $SO_2$ gases react with silver to form lubricious Ag-S components. Then, the surface wear leads to the progressive elimination of the silver and the sulfurous compounds from the interface, which explains the reduction of the sulfur concentration in the contact down to 1% at Nc. To confirm this hypothesis, XPS analysis centered at the fretting scar have been performed (Fig. 14b). XPS spectra reveal the formation of $Ag_2S$ and $Ag_2SO_4$. The resolved doublet of sulfur, at 161.4 and 162.6 eV, is a characteristic of silver sulphide $Ag_2S$ [27], as well as the signal at 168, 6 eV is a characteristic of silver sulphates $Ag_2SO_4$ [28], [29].

Both sulphide and sulphate elements are known to display very good tribological properties reducing the coefficient of friction and the wear rate [30-32] which tends to be supported by the staircase friction response observed in Figures 8 and 9. This silver sulphide & sulphate layers are very thin, about few nanometers, which in turn can explain the rather low concentration of sulfur detected by EDX analysis since this latter technique investigates a least 1 µm of the material thickness and consequently minors the [S] concentration on the top surface. A dynamic balance is thus set up between the elimination and the reformation of the tribofilm as long as the $Ag_2S$ - $Ag_2SO_4$ compounds manage to be reformed in the interface. The wear of the coating is sharply reduced and the electrical endurance increases accordingly. When the end of this balance is reached, the interface becomes similar to the one observed for non-polluted air: the friction coefficient increases and the effective wear of the coating is activated.

## 5. Discussion

The fretting wear response and the related ECR behavior of silver platted coating as a function of the relative humidity under polluted and non-polluted atmospheres can be resumed as follow:

Regarding non-polluted air situation, below the so-called $RH_{th(Air)}$=$RH_{th\_Nc(Air)}$=50% threshold relative humidity, the ECR endurance slightly increases due to a better water film lubrication

and a smooth reduction of the wear rate (Fig. 14). A powder oxide debris layer characterized by low electrical conductivity is formed promoting rather short ECR endurances.

Above $RH_{th(Air)}$ =50%, the debris layer becomes more cohesive and compacted. The silver element embedded in the third body is less easily ejected from the interface which implies a continuous decreasing of the wear rate. Furthermore, the moister debris bed is potentially more conductive. The debris thickness and therefore the wear volume $V_{Nc}$ to reach the ECR failure are increased. These combined effects (i.e. increase of the threshold wear volume and a reduction of the wear rate) explain the fast raising of the ECR endurance.

Regarding polluted air atmosphere, as long as the relative humidity remains lower than the threshold relative humidity (i.e $RH_{th(Air\&S)}$ = $RH_{th\_Nc(Air\&S)}$ = $RH_{th\_K(Air\&S)}$ = 60%) no interactions between sulfur gases and most air occur; hence, the tribological and ECR responses will be similar to the non-polled air atmosphere. Above $RH_{th(Air\&S)}$, synergic interactions between sulfur gases ([$H_2S$] =0.5 ppm and [$SO_2$] = 1.2 ppm) and moist atmosphere take place promoting the formation of a lubricious and protective Ag2S - Ag2SO4 tribofilm. When this Ag-S tribofilm is finally eliminated after $N_{LF(Air\&S)}$ fretting cycles, the effect of Ag2S - Ag2SO4 is minored and the interface response will be equivalent to that observed under equivalent RH non-polluted air configuration.

**Prediction of the ECR endurance**

Experiments and surface analysis suggest that the ECR endurance of silver plated contacts can be described considering a progressive wear-process function depending on the relative humidity and the durability of the lubricious and protective Ag-S tribolayer generated under polluted and moist atmospheres (RH> $RH_{th(Air\&S)}$ = 60%).

*Non-polluted air condition*

Regarding non-polluted air condition, the ECR endurance Nc can be approximated by coupling the threshold wear volume $V_{Nc}$ and the related wear rate K coefficient of the interface. Combining Eq.2 and 3, the ECR endurance versus relative humidity can is approximated using the following relationship:

$$Nc_{pred} = \frac{V_{Nc}(RH(\%))}{4 \times P \times \delta_S^* \times K(RH(\%))} \quad (6)$$

Fig. 10 suggests a discontinuous evolution of the $V_{Nc}$ versus the relative humidity. However, to simplify the modeling a sigmoid continuous formulation is preferred (Fig. 15a):

$$V_{Nc}(RH\%) = V_{Nc,0\%} + \left(\frac{1}{1+e^{-\lambda\times(RH(\%)-RH(\%)_{IP})}}\right) \times \left(V_{Nc,100\%} - V_{Nc,0\%}\right) \quad (7)$$

with $V_{Nc,0\%}$= 0.27 mm$^3$ the wear volume extrapolated for RH = 0%, $V_{Nc,100\%}$= 0.55 mm$^3$, the wear volume extrapolated for RH = 100%, $RH(\%)_{IP}$= 70%, inflexion point of the curve and

$\lambda$ = 0.1 the exponent of the sigmoid function.

Despite its simplicity the given expression provides a rather nice description of the experiments. Alternatively, the wear rate evolution can be approximated using a power law function (Fig. 15b):

$$K(RH\%) = C_{K,RH} \times RH(\%)^{m_{K,RH}} \quad (8)$$

with $C_{K,RH}$ = 0.06 and $m_{K,RH}$= -0.45

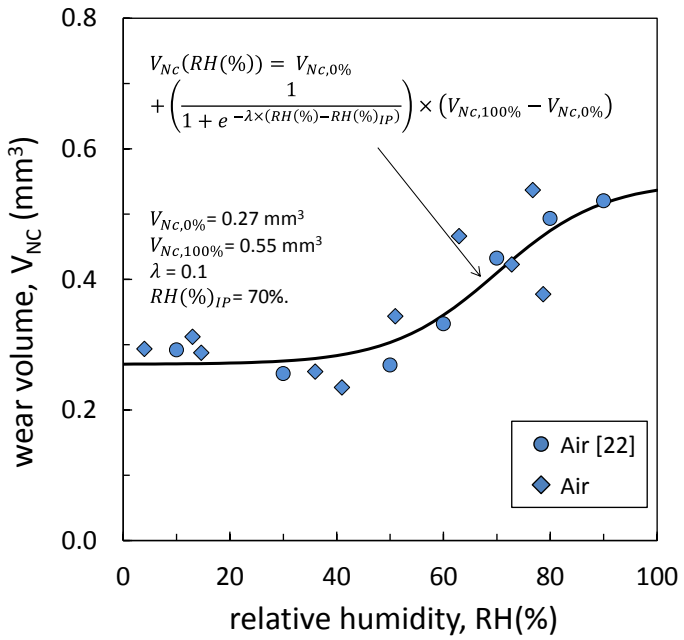


(a)

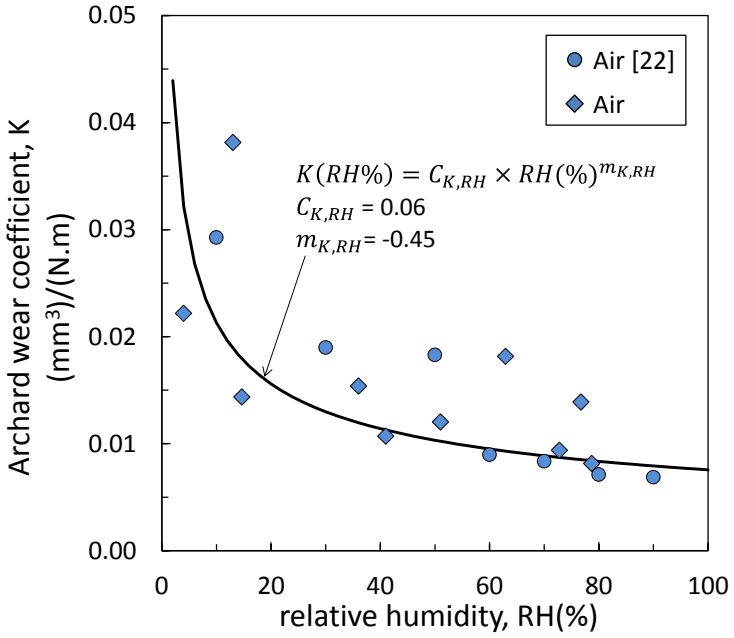


(b)

*Fig. 15 : Wear volume and wear rate evolutions versus the relative humidity under non-polluted air conditions: (a) Sigmoid approximation of $V_{NC}$ ; (b) power law approximation of the Archard wear rate K.*

By combining Eq. 6, 7 and 8, the ECR endurance versus relative humidity can be approximated using the following expression:

$$Nc_{(Air)pred} = \frac{V_{Nc,0\%}}{4 \times P \times \delta_S^* \times C_{K,RH} \times RH(\%)^{m_{K,RH}}} \times \left(1 + \left(\frac{1}{1+e^{-\lambda \times (RH(\%) - RH(\%)_{IP})}}\right) \times \left(\frac{V_{Nc,100\%}}{V_{Nc,0\%}} - 1\right)\right) \qquad (9)$$

The comparison between experimental and predicted ECR endurances displays a very nice correlation (Fig. 16). This indirectly confirms the stability of the Eq. 9 to capture the effect of the relative humidity regarding the ECR endurance under moist atmosphere.

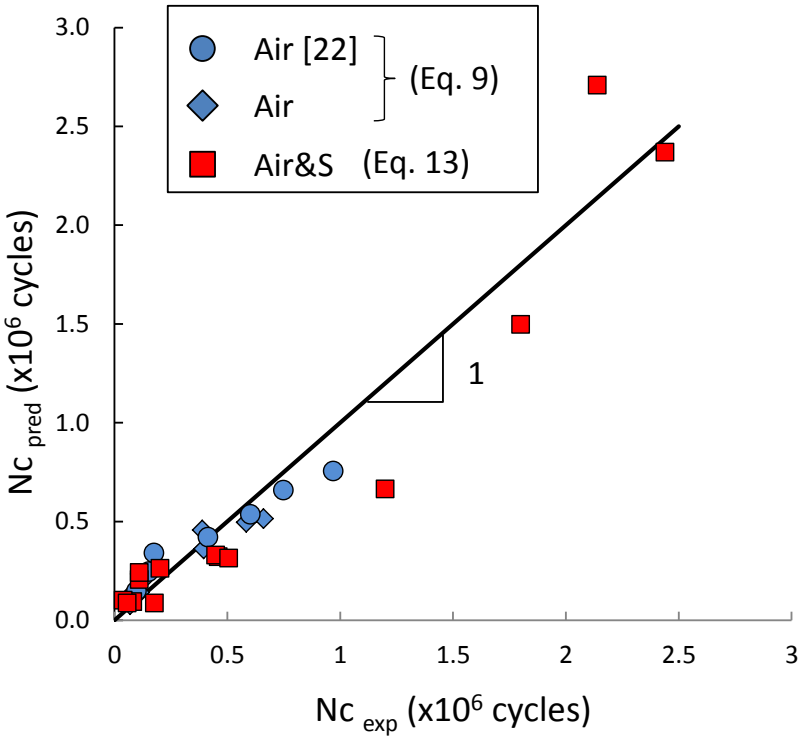


*Fig. 16: Comparison between experimental and predicted ECR endurances under non-polluted (Air) and polluted (Air&S: [$H_2S$] = 0.5 ppm and [$SO_2$] = 1.2 ppm) atmospheres varying the relative humidity from RH= 5 to 90% (P=3 N, T=25 °C, $\delta_s^*$=±9 µm, f=30 Hz).*

*Polluted air condition*

The experimental investigation suggests that the total endurance of the electrical contact under moist and polluted atmosphere can be approximated by summing the endurance related to the relative humidity effect and the endurance of the lubricious Ag2S - Ag2SO4 tribofilm:

$$Nc_{(Air\&S)} = Nc_{(Air)} + N_{LF(Air\&S)} \quad (10)$$

This assumption is confirmed by comparing the difference of ECR endurances obtained under polluted and non-polluted air conditions (Fig. 17a):

$$\Delta Nc_{(Air\&S)} = Nc_{(Air\&S)} - Nc_{(Air)} \quad (11)$$

versus the duration of the low friction plateau $N_{LF(AiR\&S)}$ measured on each friction curve (Fig. 17b). A linear correlation is observed (Fig. 17c) confirming the additive contribution of the Ag2S - Ag2SO4 tribofilm.

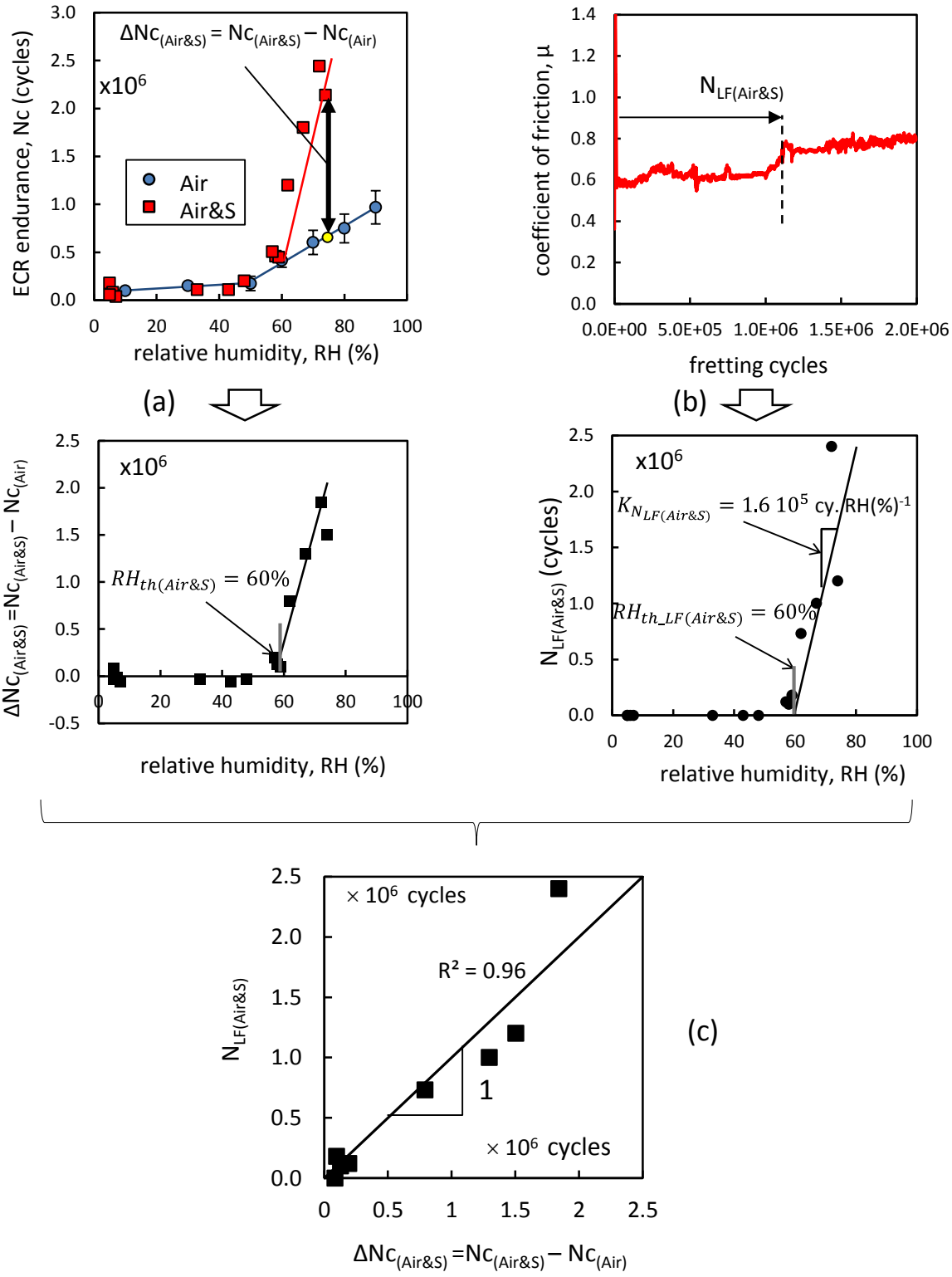


*Fig. 17: Comparison between the duration of the low friction regime, $N_{LF\ (Air\&S)}$ and the difference in endurance between the two atmospheres $\Delta Nc_{(Air\&S)} = Nc_{(Air+S)} - Nc_{(Air)}$.*

The lubricious period $N_{LF(Air\&S)}$ can therefore be estimated assuming a bilinear description (Fig. 17b):

If $RH(\%) < RH_{th(Air\&S)}$ then $N_{LF(Air\&S)pred} = 0$

If $RH(\%) > RH_{th(Air\&S)}$

then $N_{LF(Air\&S)pred} = K_{N_{LF(Air\&S)}} \times \left(RH(\%) - RH_{th(Air\&S)}\right)$ (12)

with $K_{N_{LF(Air\&S)}} = 1.6\ 10^5$ cy. RH(%)$^{-1}$

Combining Eq. 9 and 12, the predicted ECR endurance under moist and polluted air condition is given by:

$$Nc_{(Air\&S)pred} = Nc_{(Air)pred} + N_{LF(Air\&S)pred} \quad (13)$$

Figure 16 confirms a rather good correlation between predicted and experimental ECR endurances under polluted air condition. This indirectly supports the proposal and a posteriori confirms the hypothesis of an additive contribution of the Ag-S tribofilm endurance regarding the total ECR endurance of the Ag tribosystem under polluted air conditions.

**Limit and upgrading of the experimental approach**

These results are very interesting but it should be underlined that the chosen experimental protocol exhibits the tribological damage processes. In reality, an electrical contact is subjected to very long stop phases (vehicle being stopped) which can promote time dependent corrosion processes. Thus, if sulfurous gases are beneficial under fretting solicitations, they might be harmful by promoting corrosion processes. To calibrate this aspect, new protocols including long stops to reveal the silver corrosion phenomenon need to be considered in future works. Besides, the current investigation concerns a single sulfur gas composition (i.e. ([$H_2S$] = 0.5 ppm and [$SO_2$] = 1.2 ppm). There is a key interest to investigate various [$H_2S$] and [$SO_2$] concentrations at least for representative conditions of automotive or airplane engines. Finally, a key question concerns the physical interpretation of the threshold $RH_{th(Air\&S)}$ = 60% above which the $Ag_2S$-$Ag_2SO_4$ lubricious tribofilm could be formed. Why this threshold value? Does it depend on the [$H_2S$] and [$SO_2$] concentrations? Why does the endurance of $Ag_2S$-$Ag_2SO_4$ lubricious tribofilm appear a function of the relative humidity?

Finally, among all these aspects how could a variation of the [$H_2S$] and [$SO_2$] concentrations influence the activation but also the stability of the $Ag_2S$-$Ag_2SO_4$ lubricious tribofilm? Further researches are being done currently to clarify these various questions including the local measurement of the third body resistivity which appears as a key aspect to better formalize the third body properties regarding electrical contact applications. These researches will also be deepened investigating the effect of the air composition [33] but also potential palliatives like lubricants [34].

## 5. Conclusion

The following conclusions can be drawn from this investigation:

- A fretting wear test has been developed to investigate the friction, wear and electrical contact resistance (ECR) behaviors of a cross-cylinder silver-plated contact representative of automotive connector applications. This experiment allows the combined analysis of the relative humidity and the polluted air atmosphere ([$H_2S$] = 0.5 ppm and [$SO_2$] = 1.2 ppm).
- The investigation of the studied Ag/Ag interface under non-polluted air displays a bilinear increase of the ECR endurance (Nc) with the relative humidity. Below $RH_{th(Air)}$ = 50%, the latter is slow and mainly induced by a smooth water film lubrication.

Above $RH_{th(Air)}$, the ECR endurance rises faster due to the potential formation of hydrates which display a better electrical conductivity implying thicker debris bed and therefore larger $V_{Nc}$ wear volumes to reach the ECR failure condition. At the same time, a slight decrease of the wear rate, explained by the higher cohesive properties of the moist debris, is observed. These two simultaneous phenomena induce a sharp rising of the Nc ECR endurance compared to a dryer atmosphere (i.e. $RH < RH_{th(Air)}$)

- The investigation of polluted air including sulfur gases (i.e. [$H_2S$] = 0.5 ppm and [$SO_2$] = 1.2 ppm) suggests that as long as the relative humidity remains smaller than a $RH_{th(Air\&S)}$ = 60% threshold, both tribological and ECR endurance responses are similar to those detected in non-polluted air condition. Above $RH_{th(Air\&S)}$, a sharp rising of the ECR endurance compared to the non-polluted air condition is observed. Synergetic interactions between sulfur gases with Ag coating under elevated relative humidity condition ($RH > RH_{th(Air\&S)}$) lead to the formation of $Ag_2S$ sulphide and $Ag_2SO_4$ sulphate lubricious tribofilm [30, 31]. As long as this latter is operating within the fretted interface, the ECR is low and stable and ECR endurance failure is delayed in consequence. When this latter is decayed by fretting sliding (i.e. after

$N_{LF(Air\&S)}$ low friction fretting cycles), the interface returns back to an equivalent non-polluted air response. Hence, the total ECR endurance of the studied Ag/Ag interface under polluted air (with [H2S] = 0.5 ppm and [SO2] = 1.2 ppm) can be expressed as the sum of the fretting endurance under equivalent relative humidity for non-polluted air condition plus the duration of the $Ag_2S$ - $Ag_2SO_4$ lubricious tribofilm when this latter can be formed (i.e. polluted air and $RH > RH_{th(Air\&S)}$).

- Using simple analytical expressions describing the evolution of the threshold wear volume $V_{Nc}$, the fretting wear rate ($K$) and the $Ag_2S$ - $Ag_2SO_4$ tribofilm endurance ($N_{LF(Air\&S)}$), the ECR endurance Nc is estimated under polluted and non-polluted atmospheres. A good correlation with experiments confirms the stability of the proposal.

More advanced researches are now required to better calibrate the effect of corrosion phenomenon by modifying the test protocol by including long stops to exhibit the silver corrosion phenomena. More in depth investigations will be also undertaken to explain why the beneficial effect of $H_2S$ and $SO_2$ is observed above a threshold $RH_{th(Air\&S)}$= 60% and how the evolution of these contaminants can influence the nature of the interface, third body layer and finally Nc ECR endurances.

**References**


[1] M. Antler, Electrical effects of fretting materials: a review*, Wear 106 (1985) 5–33.

[2] M. Antler and M. H. Drozdowicz, Fretting corrosion of gold-plated connector contacts, Wear 74 (1981) 27–50.

[3] B. H. Chudnovsky, Degradation of Power Contacts in Industrial Atmosphere : Silver Corrosion and Whiskers, Proc. 48th IEEE Holm (2002) 140–150.

[4] M. Braunovic, Effect of intermetallic phases on the performance of tin-plated copper connections and conductors, Proc. 49th IEEE HOLM (2003) 124–131.

[5] N. Benjemaa and J. Swingler, Correlation between Wear and Electrical behaviour of contact interfaces during Fretting vibration, Proc. 23rd ICEC Conf. (2006) 215–219.

[6] S. Noël, D. Alamarguy, L. Baraton, and P. Laurat, Influence of Contact Interface Composition on the Electrical and Tribological Properties of Nickel Electrodeposits during Fretting Tests, Proc. 26th ICEC Conf. (2012).

[7] X. Liu, Z. Cai, S. Liu, J. Peng, and M. Zhu, Effect of roughness on electrical contact performance of electronic components, Microelectronics Reliability 74 (2017) 100–109

[8] F. Pompanon, J. Laporte, S. Fouvry, and O. Alquier, Normal force and displacement amplitude influences on silver-plated electrical contacts subjected to fretting wear: A basic friction energy – contact compliance formulation, Wear 426–427 (2019) 652–661.

[9] W. Ren, L. Cui, J. Chen, X. Ma, and X. Zhang, Fretting Behavior of Au Plated Copper Contacts Induced by High Frequency Vibration, Proc. 58th IEEE Holm (2012) 204–210.

[10] Y. Zhou, B. Yao, S. Ge, C. Hong, and J. Zhang, Failure Mechanism of Sliding Electrical Contacts with Various Plated Materials, Proc. 27th ICEC Conf. (2014) 108–113.

[11] H. J. Noh, J. W. Kim, S. M. Lee, and H. Jang, Effect of grain size on the electrical failure of copper contacts in fretting motion, Tribology International 111 (2017) 39–45

[12] H. Essone-Obame, L. Cretinon, B. Cousin, N. Ben Jemaa, E. Carvou, and R. El Abdi, Investigation on friction coefficient evolution for thin-gold layer contacts, Proc. 26th ICEC Conf. (2012) 411–416.

[13] M. Antler and M. H. Drozdowicz, Fretting corrosion of gold-plated connector contacts, Wear 74 (1981) 27–50.

[14] W. Ren, L. Cui, J. Chen, X. Ma, and X. Zhang, Fretting Behavior of Au Plated Copper Contacts Induced by High Frequency Vibration, Proc. 58th IEEE Holm (2012) 204–210.

[15] Å. Kassman Rudolphi and S. Jacobson, Stationary loading, fretting and sliding of silver coated copper contacts — influence of corrosion films and corrosive atmosphere, Tribol. Int. 30 (1997) 165–175.

[16] B. H. Chudnovsky, Degradation of Power Contacts in Industrial Atmosphere : Silver Corrosion and Whiskers, Proc. 48th IEEE Holm (2002) 140–150.

[17] S. Fouvry, P. Jedrzejczyk, and P. Chalandon, Introduction of an exponential formulation to quantify the electrical endurance of micro-contacts enduring fretting wear: Application to Sn, Ag and Au coatings, Wear 271 (2011) 1524–1534.

[18] S. Hannel, S. Fouvry, P. Kapsa, and L. Vincent, The fretting sliding transition as a criterion for electrical contact performance, Wear 249 (2001) 761–770

[19] A. Kassmann Rudolphi and S. Jacobson, Gross plastic fretting mechanical deterioration of silver coated electrical contacts, Wear 201 (1996) 244–254.

[20] Å. Kassman Rudolphi and S. Jacobson, Gross plastic fretting — examination of the gross weld regime, Wear 201 (1996) 255–264.

[21] J. Laporte, O. Perrinet, and S. Fouvry, Prediction of the electrical contact resistance endurance of silver-plated coatings subject to fretting wear, using a friction energy density approach, Wear 330-331 (2015) 170-181.

[22] F. Pompanon, S. Fouvry, and O. Alquier, Influence of humidity on the endurance of silver-plated electrical contacts subjected to fretting wear, Surface and Coatings Technology, 354 (2018) 246–256.

[23] S. Fouvry, Ph Kapsa and L. Vincent, Quantification of fretting damage, Wear 200 (1996) 186-205

[24] Ch. Kleber, U. Hilfrich, and M. Schreiner, In situ QCM and TM-AFM investigations of the early stages of degradation of silver and copper surfaces, Applied Surface Science 253, (2007) 3712–3721.

[25] JF. Archard, Contact and rubbing of flat surfaces. J Appl Phys 24 (1953) 981–988.

[26] P. Arnaud, S. Fouvry, and S. Garcin, A numerical simulation of fretting wear profile taking account of the evolution of third body layer, Wear, 376–377 (2017) 1475–1488.

[27] M. Doriot-Werlé, O. Banakh, P.-A. Gay, J. Matthey, and P.-A. Steinmann, Tarnishing resistance of silver–palladium thin films, *Surface and Coatings Technology* 200 (2006) 6696–6701.

[28] N. H. Turner, J. S. Murday, and D. E. Ramaker, Quantitative determination of surface composition of sulfur bearing anion mixtures by Auger electron spectroscopy, *Analytical Chemistry* 52 (1980) 84–92.

[29] V.K Kaushik, XPS core level spectra and auger parameters for some silver compounds, Journal of Electron Spectroscopy end Related Phenomena 56 (1991) 273-277.

[30] Q. Zhao and S. Bahadur, A study of the modification of the friction and wear behavior of polyphenylene sulfide by particulate Ag2S and PbTe fillers, Wear 217 (1998) 62–72.

[31] C. Schwartz and S. Bahadur, The role of filler deformability, filler–polymer bonding, and counterface material on the tribological behavior of polyphenylene sulfide (PPS), Wear 251 (2001) 1532–1540.

[32] T.E. Graedel, J.P. Franey, G.J. Gualtieri, G.W. Kammlott, D.L. Malm, On the mechanism of silver and copper sulfidation by atmospheric $H_2S$ and OCS, Corrosion Science 25 (1985) 1163-1180.

[33] J. Song, H. Yuan, V. Schinow, Fretting corrosion behavior of electrical contacts with tin coating in atmosphere and vacuum, Wear 426–427 (2019) 1439–1445

[34] S. Noel, D. Alamarguy, A. Brezard-Oudot, P. Gendre, An investigation of fretting wear behaviour of nickel coatings for electrical contacts application in dry and lubricated conditions, Wear 301(2013) 551–561